1

Observations of active galactic nuclei

The names "active galaxies" and "active galactic nuclei" (AGNs) are related to the main feature that distinguishes these objects from inactive (normal or regular) galaxies: the presence of supermassive accreting black holes (BHs) in their centers. As of 2011, there were approximately a million known sources of this type selected by their color and several hundred thousand by basic spectroscopy and accurate redshifts. It is estimated that in the local universe, at $z \leq 0.1$, about 1 out of 50 galaxies contains a fast-accreting supermassive BH, and about 1 in 3 contains a slowly accreting supermassive BH.

Detailed studies of large samples of AGNs, and the understanding of their connection with inactive galaxies and their redshift evolution, started in the late 1970s, long after the discovery of the first quasi-stellar objects (hereinafter quasars or QSOs) in the early 1960s. Although all objects containing active supermassive BHs are now referred to as AGNs, various other names, relics from the 1960s, 1970s, and even later, are still being used. Some of the names that appear occasionally in the literature, such as "Seyfert 1 galaxies" and "Seyfert 2 galaxies," in honor of Carl Seyfert, who observed the first few galaxies of this type in the late 1940s (see Chapter 6 for a detailed discussion of the various groups), are the result of an early confusion between different sources that are now known to have similar properties. The main observational difference between Seyfert 1 and Seyfert 2 galaxies is their different optical–ultraviolet (UV) spectra. Seyfert 1 galaxies show strong, very broad (2000–10,000 km s^{-1} if interpreted as Doppler broadening) permitted and semiforbidden emission lines, whereas the broadest lines in Seyfert 2 galaxies have widths that do not exceed $\sim$1200 km s^{-1}. Such differences are now interpreted as arising from different viewing angles to the centers of such sources and from a large amount of obscuration along the line of sight. The common nomenclature used throughout this book is *type-I AGNs* for those sources with unobscured lines of sight to their centers and *type-II AGNs* for objects with heavy obscuration along the line of sight that extincts basically all the optical–UV radiation from the inner parsec (pc).

Another example related to the nature of various types of AGNs was the tendency to separate AGNs according to their luminosity. The name "Seyfert galaxies" was reserved for the lower-luminosity, mostly low-redshift AGNs, whereas QSOs were considered to be the more luminous members of the family. In fact, the dividing line between Seyfert galaxies and quasars was never defined properly and is not very precise; some researchers suggest that the line should be drawn at about $L_{\rm bol} = 10^{45}$ erg s^{-1}, where $L_{\rm bol}$ is the bolometric luminosity of the central source. Others prefer a redshift-based division, for example, in some papers, all AGNs with $z \geq 0.2$ are considered quasars.

Several other names have been proposed over the years: "N-galaxies," "broad-line radio galaxies" (BLRGs), "narrow-line radio galaxies" (NLRGs), "narrow emission-line X-ray galaxies" (NLXGs), "BL-Lac objects," "optically violently variable QSOs" (OVVs), and "low-ionization nuclear emission-line regions" (LINERs), among others. The preference in this book is to use the generic name "AGNs" and to distinguish objects by their basic physical properties such as $L_{\rm bol}$, the level of ionization of the line-emitting gas, the width of emission and/or absorption lines, and the intensity of the nonthermal radiation source. A detailed discussion of the various subgroups, and general ways of classification, is given in Chapter 6.

The definition of nuclear activity in galaxies can be based either on the physical mechanism involved or on the observational signature of this activity. The physical definition is simple: an extragalactic object is considered to be an AGN if it contains a massive accreting BH in its center. The observational classification is, in many cases, not so clear because of observational limitations, because of source obscuration, and because the term *activity* covers many orders of magnitude in accretion rate. The definition adopted here is purely observational – an object is classified as an AGN if at least one of the following is fulfilled:

1. It contains a compact nuclear region emitting significantly beyond what is expected from stellar processes typical of this type of galaxy.
2. It shows the clear signature of a nonstellar continuum emitting process in its center.
3. Its spectrum contains strong emission lines with line ratios that are typical of excitation by a nonstellar radiation field.
4. It shows line and/or continuum variations.

This very broad definition extends the limits of the AGN phenomenon to objects that are not considered by all researchers to be part of this family. Moreover, given this definition, an object can leave the AGN family, and new members can be born. The former happens when the luminosity drops below a certain limit; the later occurs when a nonactive source undergoes a sudden burst of activity. The current physical model explains such cases as reflecting large changes in the accretion rate onto the BH. The subclassification of AGNs into various groups is directly related

to one of the preceding four indicators. For example, radio galaxies are AGNs because of point 2, LINERs are AGNs because of point 3, and blazars are AGNs because of point 4. All these subgroups, and others, are described in Chapter 6.

1.1. AGNs across the electromagnetic spectrum

The characteristic spectral signatures of AGNs are easily distinguished in several wavelength bands. It is customary to refer to the spectral energy distribution (SED) and describe it in terms of the monochromatic luminosity per unit frequency (L_ν erg s^{-1} Hz^{-1}), per unit energy (L_E erg s^{-1} erg^{-1}), or per unit wavelength (L_λ erg s^{-1} Å^{-1}). The equivalent monochromatic fluxes (F_ν, F_E, or F_λ) contain an additional unit of cm^{-2} and are used to describe the observed properties. Photon flux, typically used by X-ray astronomers, is discussed later. The conversion between frequency and wavelength is obtained from simple energy conservation considerations:

$$L_\nu d\nu = L_\lambda d\lambda. \tag{1.1}$$

The SED of many AGNs can be described, over a limited energy range, as

$$L_\nu \propto \nu^{-\alpha} \tag{1.2}$$

or

$$L_\lambda \propto \lambda^{-\beta}, \tag{1.3}$$

where α is the frequency spectral index, β is the wavelength spectral index, and $\beta = 2 - \alpha$. For example, the observed 1200–6000 Å continuum of many luminous AGNs is described, adequately, by $F_\nu \propto \nu^{-0.5}$ or $F_\lambda \propto \lambda^{-1.5}$. This single power-law approximation clearly fails for wavelengths below 1200 Å or above ∼6000 Å. Another example is the 2–20 keV range, where, to a good approximation, $F_E \propto E^{-0.9}$ for a large number of type-I and type-II AGNs. Examples of various SEDs covering the entire range from radio to X-ray frequencies are shown in Figure 1.1.

1.1.1. Optical–UV observations of AGNs

Optical images of luminous type-I AGNs show clear signatures of pointlike central sources with excess emission over the surrounding stellar background of their host galaxy. The nonstellar origin of these sources is determined by their SED shape and by the absence of strong stellar absorption lines. Type-II AGNs do not show such excess.

The luminosity of the nuclear, nonstellar source relative to the host galaxy luminosity can vary by several orders of magnitude. In particular, many AGNs in the local universe are much fainter than their hosts, and the stellar emission

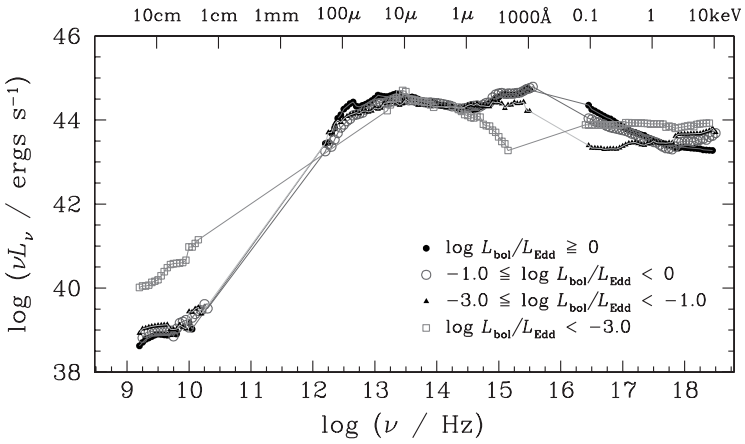

Figure 1.1. Broadband spectral energy distributions (SEDs) for various types of AGNs (from Ho, 2008; reproduced by permission of ARAA). The SEDs are normalized and do not reflect the very large range in intrinsic luminosity between different objects and different redshifts.

can dominate their total light. For example, the V-band luminosity of a high-stellar-mass AGN host can approach 10^{44} erg s^{-1}, a luminosity that far exceeds the luminosity of many local type-I AGNs. This must be taken into account when evaluating AGN spectra obtained with large-entrance-aperture instruments. The relative AGN luminosity increases with decreasing wavelength, and contamination by stellar light is not a major problem at UV wavelengths.

The optical–UV spectra shown in Figures 1.2 and 1.3 represent typical spectra of high-ionization luminous type-I and type-II AGNs. The added "high-ionization" is

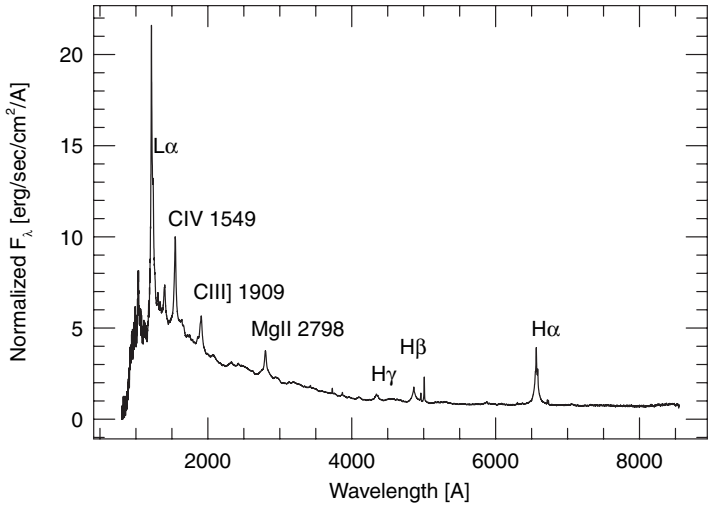

Figure 1.2. The average optical–UV SED of several thousand high-luminosity type I AGNs (adapted from data in Vanden Berk, 2001).

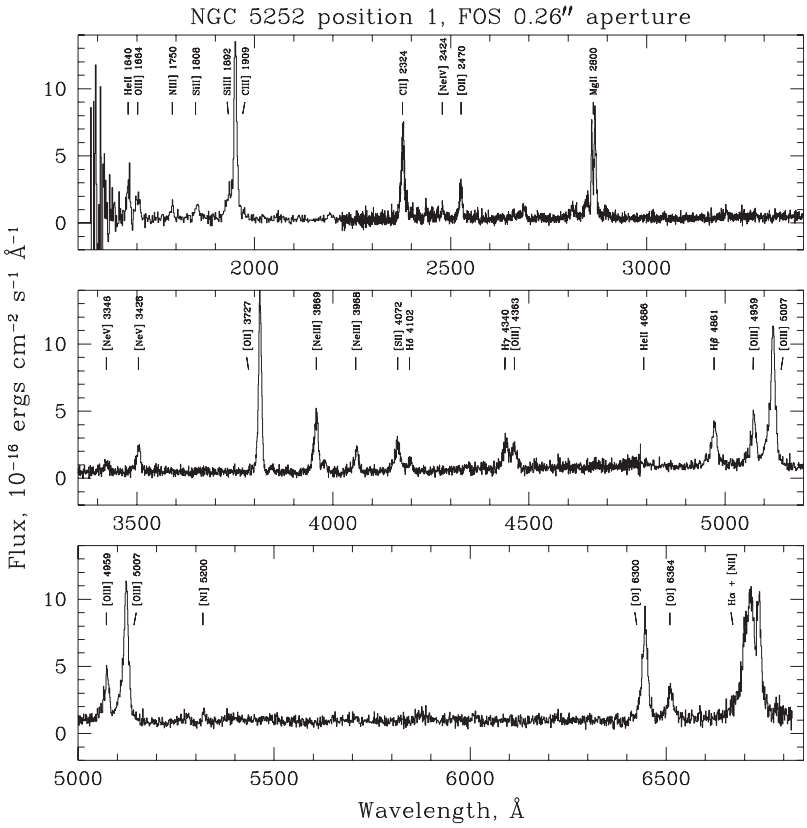

Figure 1.3. The spectrum of the low-luminosity, low-redshift type-II AGN NGC 5252 (courtesy of Zlatan Tsvetanov).

needed to distinguish such sources from low-ionization type-I and type-II sources described later. The type-I spectrum is a composite composed of several thousand spectra of different redshift AGNs. This is done to illustrate the entire rest wavelength range of 900–7000 Å using only ground-based observations. The data used to obtain this composite at $\lambda > 5000$ Å are based on spectra of lower luminosity, low-redshift objects, and the SED at those wavelengths is affected by host galaxy contamination. The type-II spectrum covers a similar range, but this time, the spectrum is a combination of a ground-based optical spectrum with a spaceborne (Hubble Space Telescope; HST) UV spectrum.

The striking differences between the high-ionization type-I and type-II spectra, which were the reason for the early classification into Seyfert 1 and Seyfert 2 galaxies, are the shape and width of the strongest emission lines. Type-II AGNs show only narrow emission lines with typical full-width-at-half-maximum (FWHM) of 400–800 km s^{-1}. In type-I spectra, all the permitted line profiles, and a few semi-forbidden line profiles, indicate large gas velocities, up to 5000–10,000 km s^{-1}

when interpreted as owing to Doppler motion. The line ratios and line widths of the forbidden lines in the spectra of type-I sources are very similar to those observed in type-II spectra and indicate that the basic physics in the narrow line-emitting region of both classes is the same. As is described in Chapter 7, the broad emission lines can be used to map the gas kinematics very close to the central BH and to measure the BH mass.

Study of the spectra of many thousand type-I AGNs shows a considerable range in optical–UV continuum slope but little if any correlation between the slope and $L_{\rm bol}$. Some of the observed differences are attributed to a small amount of reddening in the host galaxy of the AGN or other sources of foreground dust. More discussion about the origins of the SED and the effect of dust is given in Chapters 7 and 9.

Although the spectra shown here clearly illustrate the large differences in emission-line widths between type-I and type-II sources, a cautionary note is in order. Observational limitations can make it difficult to detect weak broad emission lines. Slightly obscured or low-luminosity type-I AGNs are occasionally classified as type II based on their stellarlike continua and narrow emission lines. This can be the result of reddening of the broad wings of the Hβ line or a relatively strong stellar continuum, especially in large-aperture, low-spatial-resolution observations. Higher signal-to-noise (S/N), better-spatial-resolution observations of the same sources reveal, in some cases, very broad wings in one or more Balmer lines.

The term *broad emission lines*, which is used to describe the permitted and semiforbidden lines in type-I AGNs, does not necessarily mean similar widths for all lines in all objects. The various broad emission lines show typically different widths, and in general, the width reflects the level of ionization of the gas, the source luminosity, and the mass of the central BH. Historically, it was found that broad emission lines in some type-I AGNs are narrower than narrow emission lines in type-II sources. A well-known example is the subgroup of narrow-line Seyfert 1 galaxies (NLS1s).[1] This class of objects was historically defined as those Seyfert 1 galaxies with FWHM(Hβ) < 2000 km s^{-1}. In many such sources, FWHM(Hβ) < 1000 km s^{-1}, similar to the width of Hβ in many type-II AGNs. Evidently, the distinction between type-I and type-II sources requires other criteria, such as the presence of a nonstellar continuum; strengths of emission lines typical of type-I sources such as FeII emission lines; or the presence of a strong, unobscured X-ray continuum. There are also differences in the shape and even the velocity of the same line in different objects. Some examples are shown in Figure 1.4, and more discussion is given in Chapters 5, 6, and 7.

A similar remark should be made about the width of the narrow emission lines. For example, the width of the strong [O III] λ5007 line can depend on the mass

[1] Because of these, some authors chose also to use the name "broad-line Seyfert 1 galaxies" (BLS1s) to distinguish them from the NLS1s.

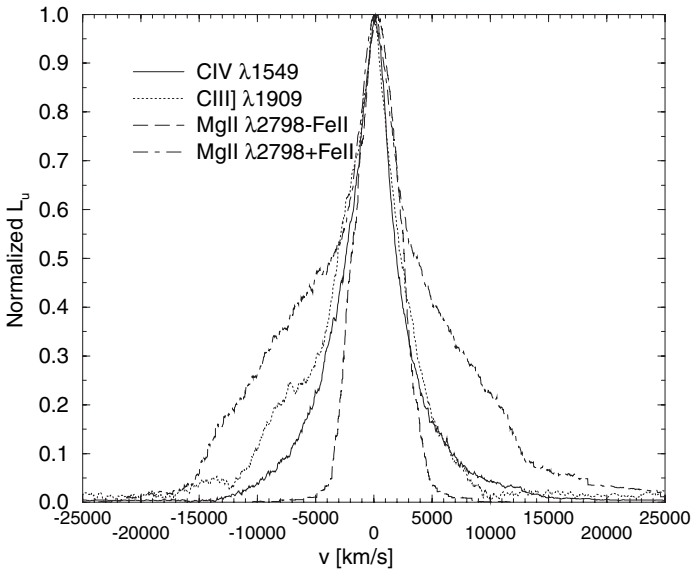

Figure 1.4. Comparison of different broad-line profiles in a typical type-I AGN.

of the central BH (or, more accurately, the mass of the bulge; see Chapter 8). Thus [O III] λ5007 lines with FWHM $\geq$ 1000 km s^{-1} are commonly observed in high-redshift, large-$M_{\rm BH}$, large-$L_{\rm bol}$ AGNs.

1.1.2. *Infrared–submillimeter observations of AGNs*

The earlier infrared (IR) observations of AGNs provided broadband photometry in the near-IR (NIR) bands, J ($\sim$1.2 μm), H ($\sim$1.6 μm), K ($\sim$2.2 μm), and L ($\sim$3.5 μm). Advances in building IR detectors and launch of IR-dedicated experiments allowed the extension of the measurements in wavelength and spectral resolution. Intermediate-resolution ($E/\Delta E$ = 1000–3000) J, H, and K spectroscopy of AGNs is now a standard procedure. Ground-based N-band ($\sim$10 μm) imaging is commonly performed, and mid-IR (MIR) spectroscopy, mostly by ISO (launched in the 1990s) and Spitzer (launched in 2003), have provided good-quality spectra of hundreds of sources, some at redshift as high as 3.

The far-IR (FIR) band of thousands of AGNs has been observed by IRAS, with limited spatial resolution, and by Spitzer, with much improved resolution. The 2009 launch of Herschel is the most recent development in this area. Broadband images with much improved spatial resolution are now available between 70 and 500 μm. Systematic surveys have already produced high-quality photometry of hundreds of AGNs and their host galaxies, up to redshift of 5 and beyond. Lower-sensitivity, high-resolution spectroscopy over the FIR range is also provided by the Herschel instruments.

Submillimeter observations of a small number of AGNs are also available, covering the range from 0.4 to about 1.2 μm. Instruments that are used in this area include SCUBA, IRAM, and other submillimeter arrays. The ALMA observatory is likely to revolutionize this area of astronomy with important implications for local as well as very high redshift AGNs.

Most of the emission in the NIR and MIR bands is due to secondary dust emission. "Secondary" in this context refers to emission by cold, warm, or hot dust grains that are heated by the primary AGN radiation source. "Primary" refers to radiation that is the direct result of the accretion process itself (Chapter 4). The temperature of the NIR- and MIR-emitting dust is between 100 and 2000 K. The dimensions of the dusty structure emitting this radiation, in intermediate luminosity AGNs, is of order 1 pc (Chapter 7). Most of the thermal FIR emission is thought to be due to colder dust that is being heated by young stars in large star-forming regions in the host galaxy (Chapter 8). In powerful radio sources, at least part of the FIR emission is due to nonthermal processes much closer to the center. Broad and narrow emission lines are seen in the NIR–FIR part of the spectrum of many AGNs. They are thought to originate in the broad- and narrow-line regions discussed in Chapter 7.

Figure 1.5 shows a composite 0.3–30 μm spectrum of intermediate-luminosity type-I AGNs. The emission longword of 1 μm is due primarily to secondary radiation from dust. The dip at 1 μm is due to the decline of the disk-produced continuum (Chapter 4) on the short-wavelength side and the rise of the emission due to hot dust on the other side.

1.1.3. X-ray observations of AGNs

X-ray images of AGNs are usually not very interesting; a point source at all X-ray energies in type-I sources and a point source in hard X-rays only in type-II AGNs. Low-resolution X-ray spectra of AGNs are available since the late 1970s. They cover the energy range from about 0.5 keV to 10 keV with a spectral resolution typical of proportional counters and CCD detectors ($\Delta E \sim 100$ eV). Using optical band terminology, these can be described as broad- or intermediate-band photometry. The situation is somewhat improved at higher energies, close to the strong 6.4 keV iron Kα line, where the resolution approaches that of low-dispersion optical spectroscopy. The Chandra and XMM-Newton missions that were launched in 1999 improved this situation dramatically by providing grating spectroscopy of nearby AGNs. The resolution of these instruments, below about 1 keV, is of order $E/\Delta E \simeq 1000$. This has revolutionized X-ray studies of AGNs and resulted in the identification of hundreds of previously unobserved emission and absorption lines. Present-day X-ray instruments like Suzaku and Swift/BAT extend the low-resolution observations to 100 keV and even beyond.

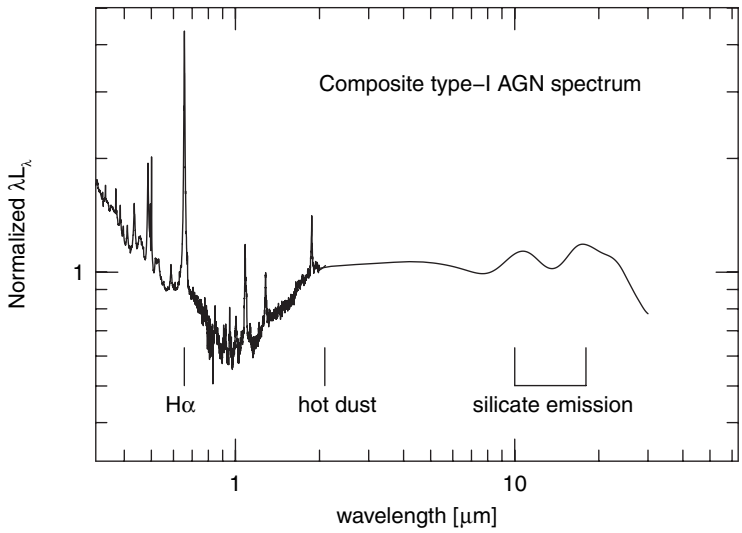

Figure 1.5. A composite spectrum of type-I AGNs covering the range 0.3–40 μm. The observations were obtained by several ground-based telescopes and Spitzer and were normalized to represent a typical intermediate-luminosity source. Note the dip at around 1 μm and the two silicate emission features around 10 and 18 μm.

The soft X-ray spectrum of many type-I AGNs is dominated by a plethora of narrow absorption lines superimposed on a strong X-ray continuum. This must represent material along the line of sight to the source. Narrow emission lines are often associated with the strongest absorption lines. X-ray spectroscopy of type-II AGNs, those with an obscured soft X-ray continuum, shows the narrow emission lines more clearly because of the attenuated central continuum. A common feature near 6.4 keV is the iron Kα line. In type-I AGN, this line is relatively weak and very broad with equivalent width (EW) of 100 eV or less. In type-II sources that are totally obscured at 6.4 keV (line-of-sight column density of $N_H = 10^{24}$ cm^{-2} or larger), the EW is much larger, 1–2 keV, and the line is narrow and barely resolved. The issue of very broad, relativistic iron-K lines is discussed in Chapter 7.

A single power law of the type $L_\nu \propto \nu^{-\alpha_X}$ fits well the intrinsic spectrum of many type-I and type-II AGNs over the energy range 0.2–20 keV. In many cases, $\alpha_X \sim 1$, but there is a clear tendency for larger α_X in objects with narrower broad emission lines. A clear example is the X-ray spectrum of NLS1s defined earlier as those type-I sources with FWHM(Hβ) < 2000 km s^{-1}.

X-ray astronomers prefer, in many cases, the use of "photon index" over "energy index." This index, Γ, is defined such that $N(E) \propto E^{-\Gamma}$, where $N(E)$ is the number of emitted photons per unit time and energy. Obviously $\Gamma = \alpha_X + 1$. The X-ray spectral index is changing with energy, and the preceding slope corresponds to a

limited range, usually 1–20 keV. There is a notable steepening of the spectrum both at much lower and much higher energies.

Another energy spectral slope, α_{ox}, is used to compare the optical–UV and X-ray luminosities of type-I AGNs. For historical reasons, the energies of comparison were chosen to be at 2500 Å and at 2 keV. The definition is

$$\alpha_{ox} = -\frac{\log L_\nu(2\,\mathrm{keV}) - \log L_\nu(2500\,\text{Å})}{2.605}. \tag{1.4}$$

Studies show that L_X/L_{UV} is luminosity dependent such that α_{ox} increases with $L_\nu(2500\,\text{Å})$. The approximate relationship is

$$\alpha_{ox} \simeq 0.114 \log L_\nu(2500\,\text{Å}) - 1.975. \tag{1.5}$$

There is a large scatter in this relationship and X-ray selection effects make the exact slope somewhat uncertain. However, it shows that the four orders of magnitude difference between low- and high-luminosity AGNs correspond to about a factor of 500 in L_X/L_{UV}. Thus the X-ray luminosity of the most luminous AGNs is only a small fraction of their total (bolometric) luminosity.

1.1.4. Radio observations of AGNs

The discovery of radio galaxies preceded the optical discovery of AGNs. It goes back to the late 1940s and the early 1950s (except, of course, for the famous paper by Seyfert from 1943). Many of these sources were later shown to have optical–UV spectra that are very similar to the various types of optically discovered AGNs. The main features of many such sources are single- or double-lobe structures with dimensions that can exceed those of the parent galaxy by a large factor and strong radio cores and/or radio jets in some sources that coincide in position with the nucleus of the optical galaxy.

Like optically classified AGNs, there are broad-line radio galaxies (BLRGs), the equivalent of the type-I sources; narrow-line radio galaxies (NLRGs), the spectroscopic equivalent of type-II AGNs; and even weak-line radio galaxies (WLRGs), the equivalent of LINERs (see Chapter 6).

While most AGNs show some radio emission, there seems to be a clear dichotomy in this property. It is therefore customary to define the "radio loudness" parameter, R, which is used to separate radio-loud from radio-quiet AGNs. R is a measure of the ratio of radio (5 GHz) to optical (B-band) monochromatic luminosity,

$$R = \frac{L_\nu(5\,\mathrm{GHz})}{L_\nu(4400\,\text{Å})} = 1.36 \times 10^5 \frac{L(5\,\mathrm{GHz})}{L(4400\,\text{Å})}, \tag{1.6}$$

below on the observations of active galactic nuclei, the exper-. iment had some more targets to explore: solar wind study, an. OH-maser monitoring, and observations of a radiostar Lambda. And. 3. Results.Â VLBI observations also reveal structures in quasar nuclei which expand at many times the speed of light. To improve VLBI observations, space-borne radiotelescopes are being examined, and the Space Shuttle is being considered for a platform and a test facility. In the future, a free-flying satellite for VLBI observations may be developed.